Ultrafast Electron Trapping at the Surface of Semiconductor Nanocrystals: Excitonic and Biexcitonic Processes

ARTICLE *in* THE JOURNAL OF PHYSICAL CHEMISTRY B · NOVEMBER 2012

Impact Factor: 3.3 · DOI: 10.1021/jp307668g · Source: PubMed

7 AUTHORS, INCLUDING:

Jonathan I Saari
ETH Zurich
13 PUBLICATIONS **157** CITATIONS
SEE PROFILE

Brenna Walsh
McGill University
15 PUBLICATIONS **102** CITATIONS
SEE PROFILE

Christopher B Murray
University of Pennsylvania
259 PUBLICATIONS **27,581** CITATIONS
SEE PROFILE

Patanjali Kambhampati
McGill University
61 PUBLICATIONS **3,104** CITATIONS
SEE PROFILE

THE JOURNAL OF PHYSICAL CHEMISTRY B

Article

pubs.acs.org/JPCB

Ultrafast Electron Trapping at the Surface of Semiconductor Nanocrystals: Excitonic and Biexcitonic Processes

Jonathan I. Saari,[†] Eva A. Dias,[†] Danielle Reifsnyder,[‡] Michael M. Krause,[†] Brenna R. Walsh,[†] Christopher B. Murray,[‡] and Patanjali Kambhampati*,[†]

[†]Department of Chemistry, McGill University, Montreal, QC, H3A 2K6, Canada

[‡]Department of Chemistry, University of Pennsylvania, Philadelphia, Pennsylvania 19104, United States

ABSTRACT: Aging of semiconductor nanocrystals (NCs) is well-known to attenuate the spontaneous photoluminescence from the band edge excitonic state by introduction of nonradiative trap states formed at the NC surface. In order to explore charge carrier dynamics dictated by the surface of the NC, femtosecond pump/probe spectroscopic experiments are performed on freshly synthesized and aged CdTe NCs. These experiments reveal fast electron trapping for aged CdTe NCs from the single excitonic state (X). Pump fluence dependence with excitonic state-resolved optical pumping enables directly populating the biexcitonic state (XX), which produces further accelerated electron trapping rates. This increase in electron trapping rate triggers coherent acoustic phonons by virtue of the ultrafast impulsive time scale of the surface trapping process. The observed trapping rates are discussed in terms of electron transfer theory.

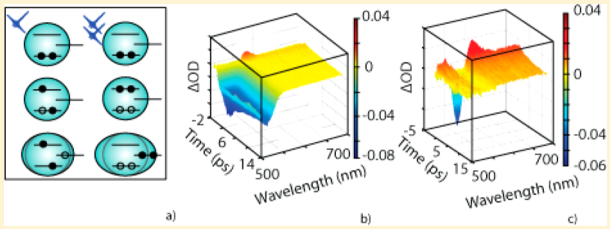

1. INTRODUCTION

Semiconductor nanocrystals (NCs) have been under intense investigation for their novel properties arising from quantum confinement.[1−9] Moreover, these properties may be exploited for a variety of device applications ranging from light emitting diodes,[10,11] optical gain and lasing,[12−17] and photovoltaics.[18] A commonly studied aspect of NC research is the structure and dynamics of quantized excitons whose behavior is dictated by the core of the NC. We use the term NC here rather than quantum dot (QD) since chemists are now able to synthesize a wide variety of semiconductor NCs[19−22] that support these confined excitons. The excitonics of the core states of NCs has been discussed in detail in recent reviews.[6−8] Specific aspects of the excitonics of NCs include electronic structure, hot exciton relaxation, multiexciton recombination and generation, exciton−phonon coupling, photoluminescence (PL), and optical gain. Despite progress in our understanding of the quantized core states of NCs, there remains a poor understanding of one of their main characteristic features: their surface.

By virtue of their size, a large fraction of the atoms in an NC are at the surface. In particular, the overlap of the excitonic wave functions with the surface of the NC becomes larger as the particle becomes smaller as anticipated from a simple hard sphere calculation. This behavior is pronounced upon inclusion of tunneling.[23−25] Hence the surface of the NC is of clear importance by simple inspection of the size of the system. This situation is unique to the NC form of the QD as their epitaxial (self-organized) variants are typically buried within a host semiconductor thereby passivating the surface.[14]

While the surface of the NC is of clear structural importance, its understanding as well as exploitation in application has lagged behind relative to the advancements in the core of the NC. The surface of the NC is largely considered to be an unwanted part of the system, with properties to be mitigated rather than engineered for use.

For example, passivating the surface is a commonly used approach to improve the PL quantum yield.[26,27] Similarly, trapping to the surface by hot excitons has been identified as a culprit in blocking optical gain in NC.[8,15,16,28] In the multiple exciton generation (MEG) or carrier multiplication (CM) process,[29−37] this hot exciton surface trapping is now becoming seen as a culprit for inconsistency in measurements of the yield of this key process.[38−46] In the MEG literature, this surface trapping process is commonly referred to as photocharging. The surface of the NC is also appearing to be a culprit in the origin of blinking in single NC PL experiments.[47−50] Hence an understanding of the manner in which the core excitonic states are coupled to the surface of the NC is of clear importance to advancing our understanding and application of these processes.

An alternative view of the surface is that it represents an opportunity to engineer the functionality of the NC, rather than merely serve as a problem to be mitigated. For example, charge extraction and injection using adsorbed molecules should involve the surface. The most common such example is the dye-sensitized NC solar cell.[51,52] Charge extraction is a key process for photovoltaic (PV) applications, with recent experiments revealing the capacity to extract multiple excitons from NC via adsorbed electron acceptors.[53−61] Whether in PV or in

Special Issue: Paul F. Barbara Memorial Issue

Received: August 2, 2012
Revised: November 27, 2012

   dx.doi.org/10.1021/jp307668g | *J. Phys. Chem. B* XXXX, XXX, XXX−XXX

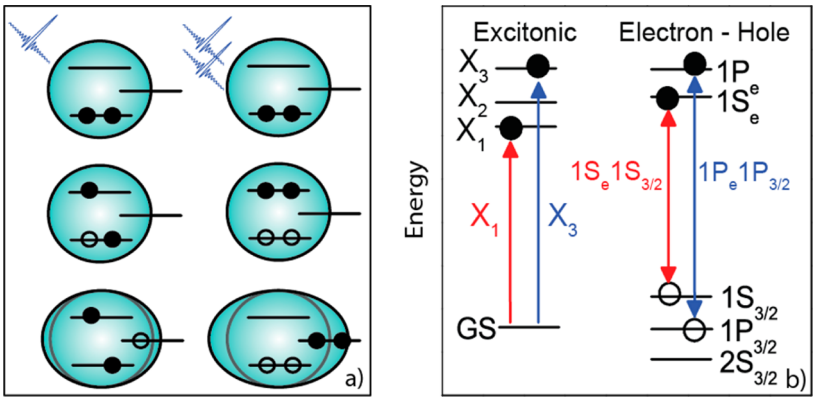

Figure 1. Schematic illustration of relevant multiexcitonic surface trapping and optical pumping processes. (a) Weak excitation conditions result in creation of a single X, which can experience either electron or hole trapping at the surface of the NC. Stronger excitation conditions result in absorption of multiple photons from a pump pulse yielding creation of an MX. (b) The electronic structure of NCs can be depicted in either the exciton or the electron/hole picture. In the excitonic picture, the lower states (e.g., X_1) are 2-fold degenerate based upon the S-type symmetries of the electron/hole states. The higher states (e.g., X_3) can have higher degeneracies, thereby supporting higher MX multiplicities.

photoconductive films, the surface of the NC should be a key factor. The surface is moreover of explicit importance for NC-based sensing[62−65] and photocatalysis applications.[66−68] Finally, the surface of small NCs is now being used as a path to generating white light-emitting NCs for LED applications.[69−76] Hence the surface is an aspect of the NC that one should engineer both to optimize certain core excitonic process such as PL, and more broadly to provide a path to optimizing surface specific processes.

In light of the importance of surface trapping in NC, one aims for additional spectroscopic signals which may assist in providing a microscopic picture of the factors which control charge trapping at the surface. In this work, we present excitonic state-resolved pump/probe data on CdTe NC as a step toward this goal. Here, we show that surface alteration during aging CdTe NC can support very fast surface trapping rates. In particular, we find fast trapping rates for electrons in aged CdTe NC. Specifically, we observe faster electron trapping for the single exciton than for fresh CdTe. In these aged CdTe samples, we find that biexcitons have enhanced surface trapping rates. The electron transfer (ET) trapping times from the ground biexcitonic state to the surface of the NC is sufficiently fast as to launch coherent acoustic phonons on the electronic ground state. These results illustrate that coherent phonons can serve as a reporter for interfacial charge transport,[77] in support of simpler decays from kinetic transients which can be ambiguous.[43] These results furthermore suggest that trapping rates may be distinct for higher multiexcitons, informing the design of acceptor systems for multiple exciton dissociation across the NC interface.[55,58−61]

2. EXPERIMENT

Synthesis. For a typical reaction, A stock tributylphosphine tellurium (TBPTe) injection solution was prepared by dissolving 0.1 g of tellurium shot (Te, Aldrich, shot 1−2 mm, 99.999%) in 2.35 mL of tributylphosphine (TBP, Aldrich, 97%) at room temperature and then diluting with 7.6 mL of 1-octadecene (ODE, Sigma-Aldrich, 90% technical grade). In a 50-mL three-neck round-bottom reaction flask, 0.0384 g (0.3 mmol) of cadmium oxide (CdO, Acros, 99%), 0.171 g (0.614 mmol) of *n*-tetradecylphosphonic acid (TDPA, Strem, ≥97%), and 15.2 mL of ODE were combined. Under nitrogen, the reaction flask was heated to 300 °C for 30 min, with a 21 gauge needle as an outlet through a septum. After 30 min, the heating mantle and outlet were removed, and 3 mL of the TBPTe stock was rapidly injected. The reaction flask was allowed to cool to room temperature with no additional heating. The samples were then dispersed in toluene after a period of roughly 72 h. In order to elucidate the effect of the surface, this work focuses on CdTe NC with radii of ∼1.5 nm. The size of the CdTe NCs was determined empirically from the wavelength of the first absorption peak.[78] The aged samples were stored in powder form for a month and redispersed in toluene. The fresh samples were not redispersed, and were used immediately.

Spectroscopy. The experimental approach used here has been discussed in our previous works.[15,16,23−25,28,43,79−85] Linear absorption and PL spectra were acquired in situ before, during, and after femtosecond experiments to ensure the absence of photodegradation. The NCs were dispersed in spectral-grade toluene and flowed through a 1 mm path length quartz flow cell via peristaltic pumping.[84] The optical density of the sample was between 100 and 200 mOD at the X_1 transition (band edge exciton). The pump pulses were derived from optical parametric amplifiers (OPAs). Pulse durations were determined via intensity autocorrelation in 30 μm of β-barium borate (BBO) and maintained at durations of between 30 and 40 fs throughout the experiment. Prism compressors were used to compensate for temporal chirp of the OPA-derived pump pulses. Pump beam waists were 300 to 400 μm. Probe pulses were obtained via single-filament white light continuum generated in a 2 mm sapphire plate. A fused silica prism compressor was used to compensate for temporal chirp of the probe. The pump pulses were chopped at 333 Hz with appropriate phase shift to acquire transients with alternating pump wavelengths at a shot by shot level.[85] The Chirp-free transient absorption (TA) spectra were acquired through a scanning monochromator.[15,16,25,80] The spectral chirp of the probe was determined via cross-correlation with the pump pulses in a 30 μm BBO crystal at the sample stage. The chirp was compensated for by simultaneously adjusting the relative pump−probe delay according to the calibrated chirp.

3. RESULTS

A. Overview. Optical excitation of the NC will create a single exciton (X) at low excitation intensity and can create multiexcitons (MX) at high intensities.[5,7,8] The simplest MX is the biexciton (XX), which is the focus of this work. One aims to measure the rate at which electrons and/or holes experience trapping to the surface of the NC[25,43,79,86−89] and the factors that

dx.doi.org/10.1021/jp307668g | J. Phys. Chem. B XXXX, XXX, XXX−XXX

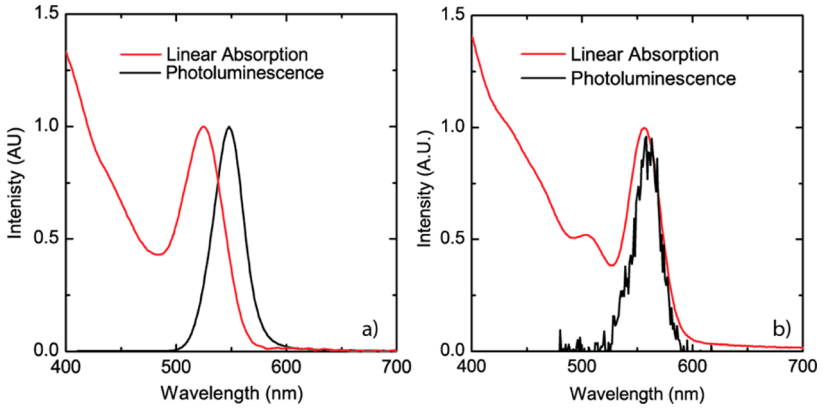

Figure 2. Linear absorption and spontaneous PL spectra of fresh (a) and aged (b) CdTe NCs. Both samples show discrete transitions in the linear absorption spectra characteristic to confined excitons in NCs. The PL from the aged CdTe has been increased by 100× for comparison.

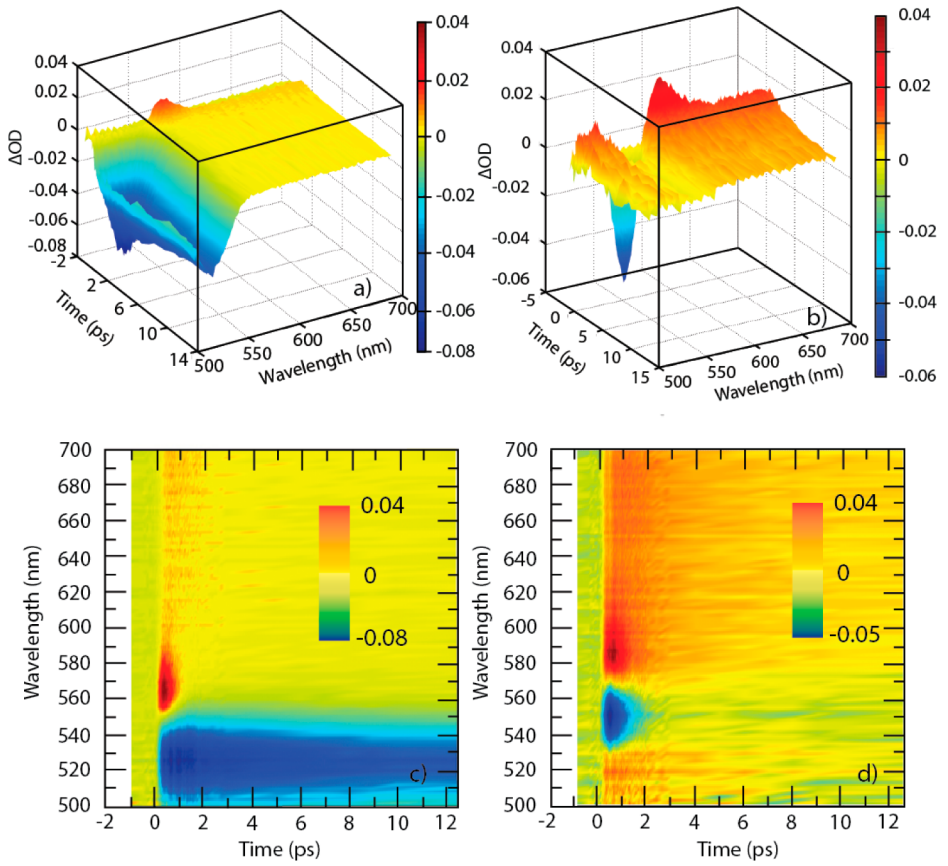

Figure 3. TA spectra of fresh (a,b) and aged (c,d) CdTe NCs shown as three-dimensional surfaces (upper panels) and contour plots (lower panels).The pump pulse was tuned to the X_3 initial excitonic state with $\langle N \rangle$ = 0.5. The main features of note are the band edge bleach signal (B1) feature, the narrowband PA (A1) feature, and the broadband PA. The aged sample shows faster decay of the B1 feature and larger amplitude of the broadband PA at the red of the TA spectrum.

govern these rates. Figure1 illustrates these processes. At low intensities, a single photon is absorbed, which creates X (Figure1a). Illustrated schematically is trapping of the hole to the surface state creating a state we previously described as a surface trapped exciton.[25,43,79] The same process is alternatively referred to as photocharging in the PL blinking and MEG/CM literature.[39,48,49,90−94] We prefer the term surface trapping, as photocharging may incorrectly lead one to consider this state as a non-neutral NC. At higher intensities, multiple photons may be absorbed,[5−8,15,16,25,28,43,80,85,95−97] thereby creating an MX state such as the XX state illustrated here. In the XX schematic, the electrons undergo surface trapping to illustrate the possibility of either carrier becoming strongly coupled to the surface of the NC.

In order to focus specifically on the XX state, one can exploit the known electronic structure of these II−VI NCs.[3,5,7,81,98,99] Commonly, one pumps at 400 nm (3.1 eV) due to convenience.[4,5] Excitation into the continuum, however, will create a Poisson distribution of MX, thereby obfuscating an excitation-dependent investigation. Recognizing the degeneracies of the excitonic states, one can spectroscopically prescribe specific MX states. Figure1b shows a schematic electronic

dx.doi.org/10.1021/jp307668g | J. Phys. Chem. B XXXX, XXX, XXX−XXX

structure of these II−VI (common to CdS, CdSe, CdTe) NC in the electron/hole as well as the exciton representation using the multiband effective mass approach.[3,98−100] The X_1 excitonic state can be described within the multiband effective mass approach as arising from a $1S_e-1S_{3/2}$ electron−hole state and the X_3 state as a $1P_e-1P_{3/2}$ electron−hole state. The key point is that the X_1 state is 2-fold degenerate, whereas the X_3 state is 6-fold degenerate. Hence pumping directly into the X_1 state rather than the continuum enables creation of an MX population with a maximum multiplicity of $\langle N\rangle = 2$. Here, $\langle N\rangle$ refers to the mean exciton occupancy.

Our prior work on CdSe revealed that a full pump/probe TA spectrum can be unraveled to identify whether it is the electron or the hole that gets trapped at the surface. We refer to our earlier works and recent reviews for more extensive discussions of the pump/probe signals.[6−8,25,28,43,80] Briefly, the band edge bleach recovery (B1 signal) monitors the electron population in the band edge exciton due to state filling. Hence, decay of the B1 signal reflects detrapping of electrons from the 1S band edge state to the surface of the NC. In contrast, the A1 signal to the red of the band edge bleach arises from absorption from X into XX and spectroscopically manifests itself as a photoinduced absorption (PA).

In the case of fresh CdSe with amine ligands, we have previously shown that the hole rather than the electron undergoes surface trapping on the 10−100 ps time scale,[25] with slower rates for larger NC as anticipated by surface fraction arguments. In those experiments, the CdSe NC were pumped directly into the band edge exciton to focus on surface trapping dynamics without obfuscation from exciton cooling. We have subsequently shown the effect of surface passivation on surface trapping in CdSe NC.[43] In those experiments, pumping into the excitonic continuum at 400 nm enabled evaluation of hot exciton surface trapping in competition with exciton cooling. Those experiments revealed that the degree of surface passivation dictates the rate of hot exciton surface trapping. In those CdSe experiments, the TA signals always revealed hole trapping to the surface.

CdTe NCs are similar in electronic structure to CdSe NCs,[100] but are less well studied.[101] Here, we evaluate the trapping dynamics of CdTe NCs as a function of sample aging. Figure 2 shows linear absorption spectra and PL spectra of the freshly synthesized as well as aged CdTe samples. Shown are representative spectra from different syntheses. The linear absorption spectra are similar to each other and to the well-known spectroscopy of CdSe NCs as anticipated from theory.

The main difference is that the aged CdTe shows very weak PL (~100x smaller than fresh CdTe) as expected from poor surface passivation due to trap states. However, it is not clear whether this aging process and passivation quality in general results in electron or hole trapping and the time scales and pathways for this charge transfer process. Hence, one aims for a more clear picture of the carrier trapping processes that take place at the surface of the NC than is afforded by simple PL measurements.

B. TA Spectra of Fresh and Aged CdTe. Figure 3 shows representative TA spectra of fresh and aged CdTe NCs with excitation into the X_3 state (1P exciton) with an excitation density of $\langle N\rangle = 0.5$. The exact transition energies between the fresh and aged samples are not identical, as they were obtained from data sets across synthetic runs. $\langle N\rangle$ refers to the mean number of absorbed photons and therefore the mean exciton occupancy. The fresh samples show TA signals qualitatively consistent with prior work on CdSe NC.[6−8,15,16,23−25,28,43,79−83,85] There is a band edge bleach in the blue that slowly recovers. Also, there is a narrowband PA immediately to the red of the band edge bleach. This narrowband PA arises from XX-induced level shifting.[6−8,25,28,80]

The TA spectra for the aged CdTe NC are qualitatively different than that of the fresh samples. In the case of the aged NCs, the B1 bleach signal recovers on the 1−2 ps time scale, orders of magnitude faster than in the fresh samples and those in CdSe. The narrowband A1 signal is considerably larger. Additionally, to the red of the A1 signal is a large broadband PA. This PA "shelf" feature has been seen by a variety of researchers,[43,95,97,102] and its origin remains unclear. We have recently assigned it as arising from intraband absorption from the quantized excitonic states into the excitonic continuum.[43] These transitions should have a large energy spectrum due to the continuum of final states thereby manifesting themselves spectroscopically as a shelf-like feature. We proposed that these transitions, not normally seen in TA spectra, become allowed by some surface trapping induced perturbation to the intraband selection rules.

C. Electron Dynamics via Band Edge Bleach. The band edge bleach recovery (B1 signal) has been well discussed initially by Klimov[4,5] and in further detail by our group.[6−8,23,24,43,81,85] This signal monitors the population of electrons in the 1S band edge exciton. We previously showed that excitation directly into X_1 yields an instrument response limited bleach by directly populating the 1S electron for the case of CdSe NC.[23,24,85] These results on CdTe show the same response (Figure 4a). Since the X_1 excitonic state has its electron already in the 1S state, there is no further relaxation that is possible within the quantized manifold of states. Hence any decay of this signal is due to electron depopulation whether via radiative recombination or ET to trap states, typically assigned as the source of nonradiative recombination.

Well passivated CdSe NCs show small amplitude decay of the B1 signal on the 30 ps time scale due to a small fraction of the NCs undergoing surface trapping on this time scale. By contrast, the CdTe NCs show faster decay and larger amplitude to the decay for both fresh and aged samples. The main observation in the B1 signal is a large amplitude to the B1 decay, thereby revealing that the aging of the NCs produces efficient electron traps at the surface of the NCs. Figure 4b,c further focuses on the B1 signals on the aged CdTe to more closely inspect the electron dynamics as determined by aging. The results on fresh CdTe samples are consistent with our prior work on CdSe[23−25,85] and will not be further discussed here. Figure 4b shows the B1 signal as a function of initial excitonic state in the manner we previously described in detail for CdSe NC using our excitonic state-resolved pump/probe approach.[6,7,23−25,85] Pumping directly into X_1-X_3 enables evaluation of state-to-state electron dynamics in these NC. Comparison of the X_1 and X_2 pumping conditions reveals identical B1 signals as we previously showed for CdSe. Hence both excitonic states share a common 1S electron state as predicted by theory. X_3 pumping shows a buildup time in a manner completely consistent with CdSe NC. These CdTe NC show a fast sub ps buildup of the B1 signal due to fast electron relaxation from 1P to 1S states. Hence, CdTe NCs also show a clear "breaking of the phonon bottleneck"[2,4] due to the presence of additional relaxation pathways.[6,7,23,24,85]

The additional relaxation pathways include Auger electron relaxation as well as ligand-based (nonadiabatic) channels. We have discussed these points in detail in our prior works and in recent reviews.[6,7,23,24,85] Upon the basis of our excitonic state-

dx.doi.org/10.1021/jp307668g | J. Phys. Chem. B XXXX, XXX, XXX−XXX

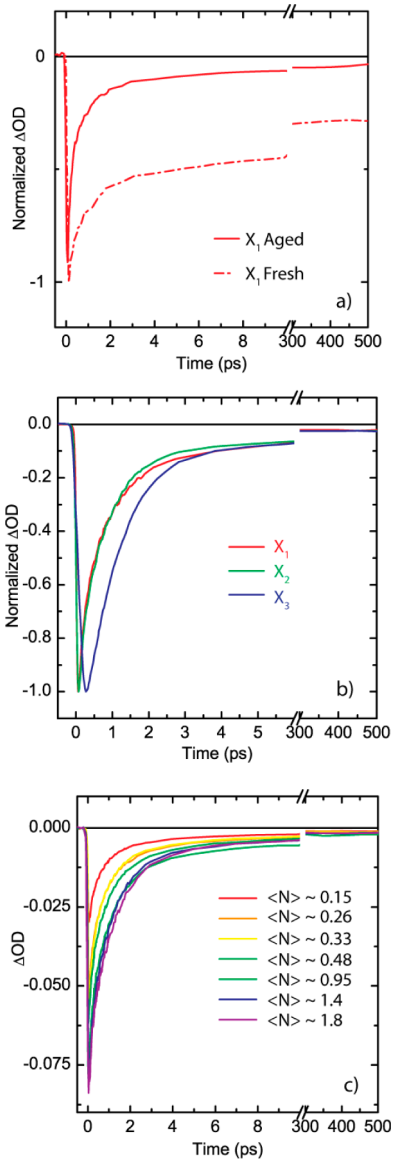

Figure 4. Femtosecond pump/probe transients, probing at the band edge exciton (B1 feature). (a) Comparison of fresh and aged samples upon pumping into X_1 or X_3. In both samples, X_3 pumping delays the buildup of the B1 feature due to hot electron relaxation. For both pumping conditions, the aged samples show a faster B1 decay. This decay arises from electron rather than hole trapping (see text for details). (b) Initial excitonic state-dependence to the B1 bleach dynamics for the aged CdTe. X_1 and X_2 pumping show identical response, indicating a common electron state. X_3 pumping shows a buildup and slowed decay due to hot electron relaxation from 1P to 1S states. (c) Pump fluence dependence to B1 dynamics for the aged sample with X_1 pumping. $\langle N \rangle$ refers to the mean exciton occupancy. $N_{max} = 2$ due to the degeneracy of the X_1 state.

resolved approach to evaluating electron/hole state-to-state transition rates, we find that the 1P → 1S electron transition takes place in 200 fs for CdTe NC (aged as well as fresh). Finally, Figure4c shows the fluence dependence to the decay of the B1 signal upon pumping directly into the 2-fold degenerate X_1 excitonic state. At higher excitation, the decay is more rapid, a point that will be discussed in detail below.

This similarity in these electron transition times between CdSe and CdTe NC is not necessarily obvious from inspection of the electronic structure of II–VI NC.[3,100] Specifically, CdTe is known to have larger spin–orbit split off for the valence band (VB) thereby decreasing the VB density of states (DOS). It is the asymmetry in the conduction band (CB) and VB DOS that enables this unidirectional electron cooling process. Hence, one might anticipate slower electron cooling for CdTe relative to CdSe NC. The similarity between the two NC suggest that the real atomistic electronic structure may still maintain a large VB DOS. Similar arguments were made by Zunger and co-workers in the case of PbSe NC.[103] In the case of PbSe, the situation is more striking in that the CB and VB are symmetric within the multiband effective mass approximation (EMA)[3,100,104−106] thereby blocking the Auger channel's requirement of larger VB DOS. In contrast, atomistic empirical pseudopotential methods[103] (EPMs) revealed that PbSe NC have a larger VB DOS, thereby maintaining their capacity for ultrafast Auger-based electron-to-hole energy transfer.

D. Hole Dynamics and XX Formation via PA Signals. Figure 5 shows the PA signals. These PA signals can be grouped in two: the now well-understood narrowband PA arising from XX-based level shifting,[5−8,25,28,80,107] and the poorly understood broadband PA "shelf" signal. TA spectra of the fresh and aged NCs are shown in Figure 5a,b, and kinetic transients are shown in Figure 5c–f. The TA spectra show clear differences for both the A1 PA as well as the shelf PA. The A1 PA arises from XX formation and enables extraction of biexciton binding energies. Here, the binding energy for the ground state (band edge) XX is 35 meV for the aged samples, qualitatively consistent with our prior works on CdSe NC.[6−8,25,28,80]

The main difference is the broadband shelf PA that is noticeable for fresh CdTe NC and very pronounced on the aged samples. This broadband PA was observed in early CdSe experiments at high intensity pumping by El-Sayed and co-workers[97] and Alivisatos and co-workers[95] as well as in recent experiments by Weiss and co-workers.[102] We previously proposed that this signal arises from a surface trapping induced perturbation to the intraband selection rules, which enables transitions from the quantized excitonic states into the continuum at high energy.[43] In fresh CdSe, the samples had to be degraded by illumination in order to produce the broadband PA due to surface trapping. By contrast, the fresh CdTe NCs show this surface trapping signal readily. Additionally, the aged CdTe NCs show this signal with still greater amplitude. We use this broadband PA as a spectroscopic signature of carrier trapping at the surface of the NC. In the case of our prior CdSe work,[25] it was straightforward to assign this PA as arising from hole trapping. Here, such analysis is complicated by the presence of electron as well as hole trapping. These TA spectra that focus upon the PA signals clearly show that there is efficient surface trapping in CdTe, and this trapping is further enhanced due to aging.

E. Coherent Phonons. We have previously explored the excitonic state-dependence of the coupling of longitudinal optical (LO) and acoustic (LA) phonons in CdSe NC.[6,7,82,83] In particular, those results revealed specific excitonic state-dependence to optically excited coherent phonons in NCs. Subsequently, we found that an additional nonoptical carrier dynamics-based mechanism can as well prepare coherent phonons.[79] Specifically, hot exciton surface trapping in photo-treated CdSe created large amplitude coherent acoustic phonons by vibrationally impulsive hole capture at the surface of the NC. This hole capture creates a large piezoelectric effect across the NC interface, thereby coupling the LA phonons.[79] Hence the observation of coherent phonons may serve as a marker for

dx.doi.org/10.1021/jp307668g | J. Phys. Chem. B XXXX, XXX, XXX–XXX

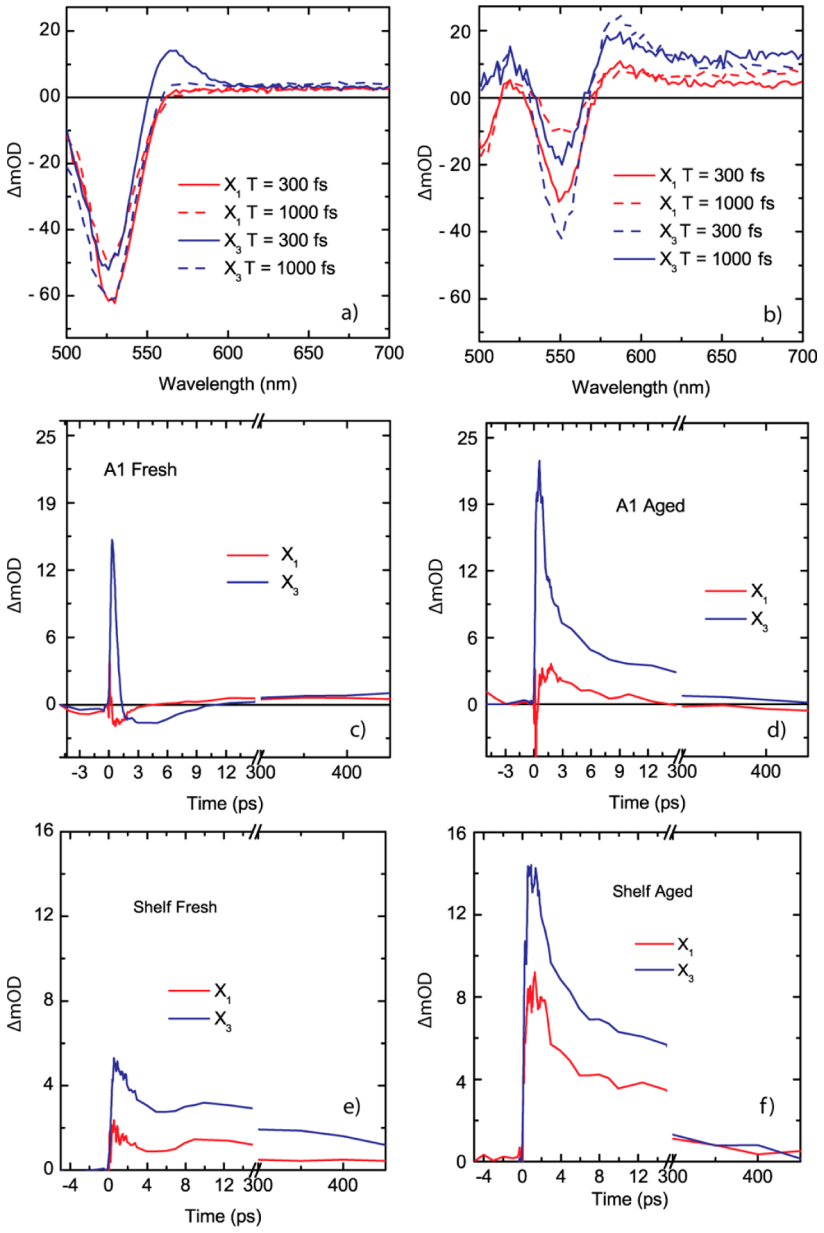

Figure 5. TA spectra of fresh (a) and aged (b) samples with X_1 and X_3 pump at t = 100/300/1000 fs. Femtosecond pump/probe transients, probing at the narrowband PA (A1 feature) for fresh (λ_{probe} = 564 nm) (c) and aged (λ_{probe} = 577 nm) (d) samples. Femtosecond pump/probe transients, probing at the broadband PA (λ_{probe} = 661 nm) for fresh (e) and aged (f) samples.

carrier dynamics (e.g., trapping),[77,79] in addition to their more common use as means to evaluate exciton−phonon coupling via optical excitation.[82,83,108]

These experiments reveal that coherent optical and acoustic phonons are launched as revealed in the oscillations in the TA spectra. Subtraction of the nonoscillatory signal reveals the coherent phonons in detail (Figure 6). Figure 6a shows the state-dependence to the coherent oscillations for the first three excitonic states with an exciton density of $\langle N \rangle$ = 0.5 and probing at the peak of the derivative of the linear absorption spectrum. Figure 6b shows the fast Fourier transform (FFT) spectrum of these oscillations, thereby showing simultaneous observation of both modes, enabling analysis of the manner in which they are excited as well as their coupling strengths. The coherent phonons show a clear state-dependence that is consistent with our prior work.[82,83] Specifically, higher excitonic states do not reveal coherent LO phonons but do reveal the coherent LA phonons. The fluence dependence with excitation into the 1S type band edge exciton (X_1) reveals that the relative intensities do not scale equally (Figure 6c). Specifically, the LA intensity increases, whereas the LO intensity saturates as discussed below.

4. DISCUSSION: EXCITATION-INDUCED SURFACE TRAPPING DYNAMICS

Whereas high-quality CdSe NCs passivated by organic ligands have been available for some time, a counterpart for CdTe has proved difficult to achieve, due to the presumed poorer surface quality of CdTe NCs. Surface quality is further degraded during the course of aging. Hence, one aims for spectroscopic signatures of surface trapping as well as aging so as to characterize the surface quality of the system as well as the ways in which surface conditions can dictate carrier relaxation and migration processes.

dx.doi.org/10.1021/jp307668g | J. Phys. Chem. B XXXX, XXX, XXX−XXX

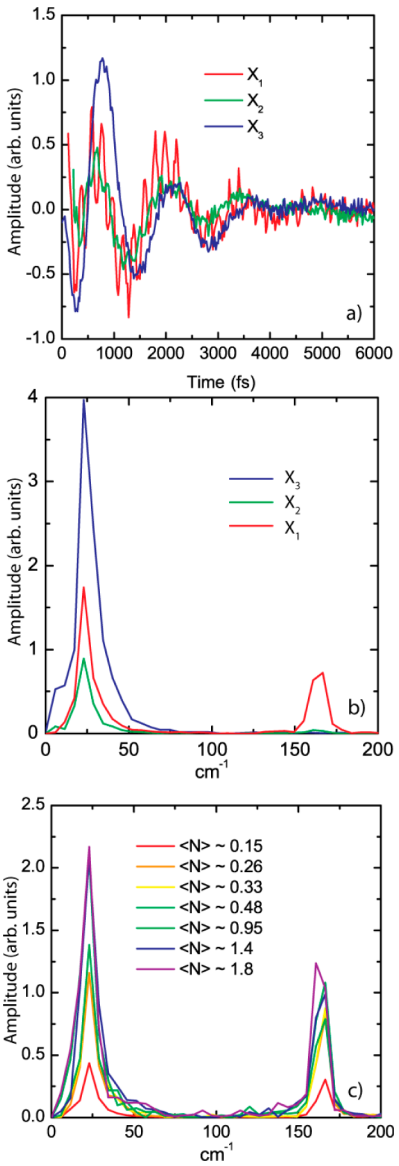

Figure 6. Real-time observation of coherent phonons as a direct measure of fast carrier trapping. (a) Initial excitonic state-dependence to the residual oscillations in the B1 transients for the aged CdTe. (b) FFT of the oscillations recovers the high-frequency optical and the low-frequency acoustic phonons. X_1 pumping uniquely enables simultaneous observation of both optical and acoustic phonons. (c) Excitation dependence to phonon spectra with X_1 pumping of aged CdTe.

Below we suggest how these various spectroscopic signals are connected via a simple ET picture.

The band edge bleach (B1 signal) decays in these aged CdTe NCs with a faster response than in fresh CdTe and CdSe NCs. The decay at all fluences is well fit to a biexponential with two time constants (Figure 7a). The slow time constant of $T_1 \sim 1.3$ ps is fairly independent of excitation conditions. By contrast, the fast component, T_2, monotonically decreases with fluence. The oscillation amplitudes of the LO and LA phonons also show a fluence dependence, represented by the mean occupancy, $\langle N \rangle$. Figure 7b shows the ratio of the LA/LO amplitudes thereby using ratiometry of the oscillations as measure of any carrier trapping dynamics induced mechanism by which the phonons are triggered. The LA/LO ratio increases monotonically with $\langle N \rangle$, much like the fast B1 decay component thereby suggesting correlation. Such a correlation between electron trapping and acoustic phonon coupling may be consistent with a simple ET picture of surface trapping. Similar correlations were recently observed by Wachtvietl and co-workers for coherent optical phonons triggered by ultrafast ET to adsorbed molecules.[77]

In a Marcus-type ET picture,[109] population transfer between the excitonic states and a surface trapped state implies a thermally activated process by which electrons and/or holes are transported from their excitonic core states to some surface state. Recent work by Jones and Scholes[110−112] has confirmed the applicability of this classically activated transport process as revealed by the temperature dependence of the PL decay times in CdSe-based NCs. We have recently[113] extended this classical Marcus picture to a semiclassical Marcus−Jortner ET picture,[109] which can explain the temperature dependence of the trap PL as well as the excitonic PL. The relevant point is that a classical activation barrier will produce a constraint on the rate at which surface trapping takes place. For CdSe NC, we showed that surface trapping takes place on the 10−100 ps time scale.[25] By contrast, electron trapping from the band edge exciton in these aged CdTe NCs takes place on the time scale of 2 ps. This picture enables rationalization of the coherent phonon response. At high fluence, sequential absorption from the X to the XX yields a state at high total energy. The total energy is twice the exciton energy minus the XX binding energy, $E_{XX} = 2E_X - \Delta_{XX}$.[7,8,25,28,80] With this amount of excess energy, the ET reaction can proceed in a barrierless manner,[109] thereby increasing the trapping rate (see Figure 8). The phenomenology of trap PL consistently reveals that it becomes more prominent at low temperatures.[113−115] Our recent work provides a quantitative treatment of these observations in light of semiclassical Marcus−Jortner ET theory.[113] Qualitatively, one expects a barrier of $\sim kT$ due to the temperature dependence of the trap PL over the range of 10−300 K. With a electron trapping time from the single exciton taking place in ~1.3 ps, barrier removal by absorption into XX predicts a trapping time of 200−300 fs, thereby rationalizing these observations.

5. CONCLUSIONS

Aging of semiconductor NCs is well-known to reduce the PL intensity by creating nonradiative traps at the surface. These simple PL experiments do not reveal the microscopic details by which the surface conditions dictate carrier relaxation and trapping processes. These femtosecond pump/probe experiments on fresh and aged CdTe semiconductor NCs reveal a variety of carrier dynamical processes and the way in which they are influenced by the surface of the NCs due to aging. We find that many of the core exciton dynamics of fresh and aged CdTe are consistent with CdSe NCs: fast electron relaxation, thereby breaking the phonon bottleneck, and strongly bound XXs. In addition, we find specific surface trapping related processes that arise due to aging of the NCs. Specifically, aging alters the surface so as to produce efficient electron traps. These electron traps at the surface of the NCs become more efficient for higher states, e.g., the biexcitons probed here. We find that trapping from the biexcitonic state is sufficiently rapid as to trigger coherent acoustic phonons as revealed in the pump/probe transients. These experiments reveal that a rich manifold of signals available in pump/probe spectroscopy can be used to characterize surface trapping processes in semiconductor NCs.

dx.doi.org/10.1021/jp307668g | J. Phys. Chem. B XXXX, XXX, XXX−XXX

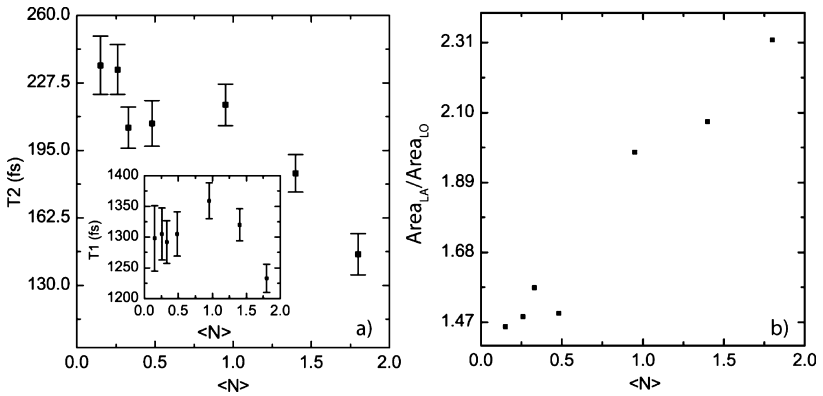

Figure 7. Pump fluence dependence reveals a relation between the decay time and coherent phonon response in terms of the mean exciton occupancy, $\langle N \rangle$. (a) Fluence dependence to the fast component of the B1 decay of aged CdTe with X_1 pumping. The inset shows the slow component has no fluence dependence. (b) Fluence dependence to the ratio of the integrated areas for the LA/LO phonons.

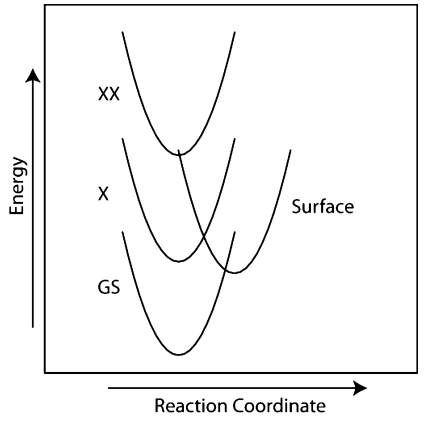

Figure 8. Schematic illustration of surface trapping in an ET scheme. Charge carrier trapping (electron or hole) from X to the surface as an activated ET process. A biexciton (XX) has higher total energy ($E_{XX} = 2E_X - \Delta_{XX}$), with Δ_{XX} representing the biexciton binding energy. At high energy the ET reaction to the surface of the NC can be barrierless thereby increasing its rate.

AUTHOR INFORMATION

Corresponding Author

*E-mail: pat.kambhampati@mcgill.ca.

Notes

The authors declare no competing financial interest.

ACKNOWLEDGMENTS

Financial support from CFI, NSERC, and FQRNT is acknowledged. E.A.D. acknowledges fellowship support from NSERC.

REFERENCES

(1) Alivisatos, A. P. *Science* **1996**, *271*, 933−937.
(2) Nozik, A. J. *Annu. Rev. Phys. Chem.* **2001**, *52*, 193−231.
(3) Efros, A. L.; Rosen, M. *Annu. Rev. Mater. Sci.* **2000**, *30*, 475−521.
(4) Klimov, V. I. *J. Phys. Chem. B* **2000**, *104*, 6112−6123.
(5) Klimov, V. I. *Annu. Rev. Phys. Chem.* **2007**, *58*, 635−673.
(6) Kambhampati, P. *J. Phys. Chem. C* **2011**, *115*, 22089−22109.
(7) Kambhampati, P. *Acc. Chem. Res.* **2011**, *44*, 1−13.
(8) Kambhampati, P. *J. Phys. Chem. Lett.* **2012**, *3*, 1182−1190.
(9) Scholes, G. D.; Rumbles, G. *Nat. Mater.* **2006**, *5*, 683−696.
(10) Coe, S.; Woo, W.-K.; Bawendi, M.; Bulovic, V. *Nature* **2002**, *420*, 800−803.
(11) Rogach, A. L.; Gaponik, N.; Lupton, J. M.; Bertoni, C.; Gallardo, D. E.; Dunn, S.; Li Pira, N.; Paderi, M.; Repetto, P.; Romanov.; et al. *Angew. Chem., Int. Ed.* **2008**, *47*, 6538−6549.
(12) Klimov, V. I.; Ivanov, S. A.; Nanda, J.; Achermann, M.; Bezel, I.; McGuire, J. A.; Piryatinski, A. *Nature* **2007**, *447*, 441−446.
(13) Klimov, V. I.; Mikhailovsky, A. A.; Xu, S.; Malko, A.; Hollingsworth, J. A.; Leatherdale, C. A.; Eisler, H.; Bawendi, M. G. *Science* **2000**, *290*, 314−317.
(14) Kambhampati, P.; Mi, Z.; Cooney Ryan, R. Colloidal and Self-Assembled Quantum Dots for Optical Gain. In *Comprehensive Nanoscience and Technology*; Andrews, D. L., Scholes, G. D., Wiederrecht, G. P., Eds.; Academic Press: Oxford, U.K., 2011; Vol. *1*, pp 493−542.
(15) Cooney, R. R.; Sewall, S. L.; Sagar, D. M.; Kambhampati, P. *J. Chem. Phys.* **2009**, *131*, 164706.
(16) Cooney, R. R.; Sewall, S. L.; Sagar, D. M.; Kambhampati, P. *Phys. Rev. Lett.* **2009**, *102*, 127404−127404.
(17) Dias, E. A.; Saari, J. I.; Tyagi, P.; Kambhampati, P. *J. Phys. Chem. C* **2012**, *116*, 5407−5413.
(18) Gur, I.; Fromer, N. A.; Geier, M. L.; Alivisatos, A. P. *Science* **2005**, *310*, 462−465.
(19) Saba, M.; Minniberger, S.; Quochi, F.; Roither, J.; Marceddu, M.; Gocalinska, A.; Kovalenko, M. V.; Talapin, D. V.; Heiss, W.; Mura, A.; Bongiovanni, G. *Adv. Mater.* **2009**, *21*, 4942−4946.
(20) Talapin, D. V.; Nelson, J. H.; Shevchenko, E. V.; Aloni, S.; Sadtler, B.; Alivisatos, A. P. *Nano Lett.* **2007**, *7*, 2951−2959.
(21) Kazes, M.; Oron, D.; Shweky, I.; Banin, U. *J. Phys. Chem. C* **2007**, *111*, 7898−7905.
(22) Avidan, A.; Oron, D. *Nano Lett.* **2008**, *8*, 2384−2387.
(23) Cooney, R. R.; Sewall, S. L.; Dias, E. A.; Sagar, D. M.; Anderson, K. E. H.; Kambhampati, P. *Phys. Rev. B* **2007**, *75*, 245311−245314.
(24) Cooney, R. R.; Sewall, S. L.; Anderson, K. E. H.; Dias, E. A.; Kambhampati, P. *Phys. Rev. Lett.* **2007**, *98*, 177403−177404.
(25) Sewall, S. L.; Cooney, R. R.; Anderson, K. E. H.; Dias, E. A.; Sagar, D. M.; Kambhampati, P. *J. Chem. Phys.* **2008**, *129*, 084701.
(26) Hines, M. A.; Guyot-Sionnest, P. *J. Phys. Chem.* **1996**, *100*, 468−471.
(27) Dabbousi, B. O.; Rodriguez-Viejo, J.; Mikulec, F. V.; Heine, J. R.; Mattoussi, H.; Ober, R.; Jensen, K. F.; Bawendi, M. G. *J. Phys. Chem. B* **1997**, *101*, 9463−9475.
(28) Sewall, S. L.; Cooney, R. R.; Dias, E. A.; Tyagi, P.; Kambhampati, P. *Phys. Rev. B* **2011**, *84*, 235304.
(29) Schaller, R. D.; Pietryga, J. M.; Klimov, V. I. *Nano Lett.* **2007**, *7*, 3469−3476.
(30) Klimov, V. I. *J. Phys. Chem. B* **2006**, *110*, 16827−16845.
(31) Franceschetti, A.; An, J. M.; Zunger, A. *Nano Lett.* **2006**, *6*, 2191−2195.
(32) Schaller, R. D.; Agranovich, V. M.; Klimov, V. I. *Nat. Phys.* **2005**, *1*, 189−194.

(33) Schaller, R. D.; Klimov, V. I. *Phys. Rev. Lett.* **2004**, *92*, 186601/186601−186601/186604.
(34) Nozik, A. J.; Beard, M. C.; Luther, J. M.; Law, M.; Ellingson, R. J.; Johnson, J. C. *Chem. Rev.* **2010**, *110*, 6873−6890.
(35) Nozik, A. J. *Chem. Phys. Lett.* **2008**, *457*, 3−11.
(36) Beard, M. C.; Knutsen, K. P.; Yu, P. R.; Luther, J. M.; Song, Q.; Metzger, W. K.; Ellingson, R. J.; Nozik, A. J. *Nano Lett.* **2007**, *7*, 2506−2512.
(37) Ellingson, R. J.; Beard, M. C.; Johnson, J. C.; Yu, P. R.; Micic, O. I.; Nozik, A. J.; Shabaev, A.; Efros, A. L. *Nano Lett.* **2005**, *5*, 865−871.
(38) Nair, G.; Chang, L.-Y.; Geyer, S. M.; Bawendi, M. G. *Nano Lett.* **2011**, *11*, 2145−2151.
(39) McGuire, J. A.; Sykora, M.; Joo, J.; Pietryga, J. M.; Klimov, V. I. *Nano Lett.* **2010**, *10*, 2049−2057.
(40) Trinh, M. T.; Houtepen, A. J.; Schins, J. M.; Hanrath, T.; Piris, J.; Knulst, W.; Goossens, A.; Siebbeles, L. D. A. *Nano Lett.* **2008**, *8*, 1713−1718.
(41) Nair, G.; Geyer, S. M.; Chang, L. Y.; Bawendi, M. G. *Phys. Rev. B* **2008**, *78*, 125325.
(42) Ben-Lulu, M.; Mocatta, D.; Bonn, M.; Banin, U.; Ruhman, S. *Nano Lett.* **2008**, *8*, 1207−1211.
(43) Tyagi, P.; Kambhampati, P. *J. Chem. Phys.* **2011**, *134*, 094706−094710.
(44) Trinh, M. T.; Polak, L.; Schins, J. M.; Houtepen, A. J.; Vaxenburg, R.; Maikov, G. I.; Grinbom, G.; Midgett, A. G.; Luther, J. M.; Beard, M. C.; et al. *Nano Lett.* **2011**, *11*, 1623−1629.
(45) Beard, M. C.; Midgett, A. G.; Law, M.; Semonin, O. E.; Ellingson, R. J.; Nozik, A. J. *Nano Lett.* **2009**, *9*, 836−845.
(46) Gdor, I.; Sachs, H.; Roitblat, A.; Strasfeld, D. B.; Bawendi, M. G.; Ruhman, S. *ACS Nano* **2012**, *6*, 3269−3277.
(47) Cordones, A. A.; Bixby, T. J.; Leone, S. R. *J. Phys. Chem. C* **2011**, *115*, 6341−6349.
(48) Zhao, J.; Nair, G.; Fisher, B. R.; Bawendi, M. G. *Phys. Rev. Lett.* **2010**, *104*, 157403.
(49) Rosen, S.; Schwartz, O.; Oron, D. *Phys. Rev. Lett.* **2010**, *104*, 157404.
(50) Peterson, J. J.; Nesbitt, D. J. *Nano Lett.* **2009**, *9*, 338−345.
(51) Kamat, P. V. *J. Phys. Chem. C* **2008**, *112*, 18737−18753.
(52) Kamat, P. V. *J. Phys. Chem. C* **2007**, *111*, 2834−2860.
(53) Zhu, H. M.; Song, N. H.; Lian, T. Q. *J. Am. Chem. Soc.* **2010**, *132*, 15038−15045.
(54) Jin, S. Y.; Hsiang, J. C.; Zhu, H. M.; Song, N. H.; Dickson, R. M.; Lian, T. Q. *Chem. Sci.* **2010**, *1*, 519−526.
(55) Huang, J.; Huang, Z. Q.; Yang, Y.; Zhu, H. M.; Lian, T. Q. *J. Am. Chem. Soc.* **2010**, *132*, 4858−4864.
(56) Boulesbaa, A.; Huang, Z. Q.; Wu, D.; Lian, T. Q. *J. Phys. Chem. C* **2010**, *114*, 962−969.
(57) Jin, S. Y.; Lian, T. Q. *Nano Lett.* **2009**, *9*, 2448−2454.
(58) Yang, Y.; Rodríguez-Córdoba, W.; Lian, T. *Nano Lett.* **2012**, *12*, 4235−4241.
(59) Zhu, H.; Lian, T. *J. Am. Chem. Soc.* **2012**, *134*, 11289−11297.
(60) Zhu, H.; Song, N.; Rodríguez-Córdoba, W.; Lian, T. *J. Am. Chem. Soc.* **2012**, *134*, 4250−4257.
(61) Zhu, H.; Song, N.; Lian, T. *J. Am. Chem. Soc.* **2011**, *133*, 8762−8771.
(62) Krooswyk, J. D.; Tyrakowski, C. M.; Snee, P. T. *J. Phys. Chem. C* **2010**, *114*, 21348−21352.
(63) Snee, P. T.; Tyrakowski, C. M.; Page, L. E.; Isovic, A.; Jawaid, A. M. *J. Phys. Chem. C* **2011**, *115*, 19578−19582.
(64) Thakar, R.; Chen, Y.; Snee, P. T. *Nano Lett.* **2007**, *7*, 3429−3432.
(65) Snee, P. T.; Somers, R. C.; Nair, G.; Zimmer, J. P.; Bawendi, M. G.; Nocera, D. G. *J. Am. Chem. Soc.* **2006**, *128*, 13320−13321.
(66) Lee, K.; Tienes, B. M.; Wilker, M. B.; Schnitzenbaumer, K. J.; Dukovic, G. *Nano Lett.* **2012**, *12*, 3268−3272.
(67) Brown, K. A.; Wilker, M. B.; Boehm, M.; Dukovic, G.; King, P. W. *J. Am. Chem. Soc.* **2012**, *134*, 5627−5636.
(68) Zhu, H.; Song, N.; Lv, H.; Hill, C. L.; Lian, T. *J. Am. Chem. Soc.* **2012**, *134*, 11701−11708.
(69) Schreuder, M. A.; McBride, J. R.; Dukes, A. D.; Sammons, J. A.; Rosenthal, S. J. *J. Phys. Chem. C* **2009**, *113*, 8169−8176.
(70) Bowers, M. J.; McBride, J. R.; Garrett, M. D.; Sammons, J. A.; Dukes, A. D.; Schreuder, M. A.; Watt, T. L.; Lupini, A. R.; Pennycook, S. J.; Rosenthal, S. J. *J. Am. Chem. Soc.* **2009**, *131*, 5730−+.
(71) Schreuder, M. A.; Gosnell, J. D.; Smith, N. J.; Warnement, M. R.; Weiss, S. M.; Rosenthal, S. J. *J. Mater. Chem.* **2008**, *18*, 970−975.
(72) Dukes, A. D.; Schreuder, M. A.; Sammons, J. A.; McBride, J. R.; Smith, N. J.; Rosenthal, S. J. *J. Chem. Phys.* **2008**, *129*, 121102.
(73) Pennycook, T. J.; McBride, J. R.; Rosenthal, S. J.; Pennycook, S. J.; Pantelides, S. T. *Nano Lett.* **2012**, *12*, 3038−3042.
(74) Rosson, T. E.; Claiborne, S. M.; McBride, J. R.; Stratton, B. S.; Rosenthal, S. J. *J. Am. Chem. Soc.* **2012**, *134*, 8006−8009.
(75) Dukes, A. D.; Samson, P. C.; Keene, J. D.; Davis, L. M.; Wikswo, J. P.; Rosenthal, S. J. *J. Phys. Chem. A* **2011**, *115*, 4076−4081.
(76) Schreuder, M. A.; Xiao, K.; Ivanov, I. N.; Weiss, S. M.; Rosenthal, S. J. *Nano Lett.* **2010**, *10*, 573−576.
(77) Dworak, L.; Matylitsky, V. V.; Braun, M.; Wachtveitl, J. *Phys. Rev. Lett.* **2011**, *107*, 247401.
(78) Yu, W. W.; Qu, L.; Guo, W.; Peng, X. *Chem. Mater.* **2003**, *15*, 2854−2860.
(79) Tyagi, P.; Cooney, R. R.; Sewall, S. L.; Sagar, D. M.; Saari, J. I.; Kambhampati, P. *Nano Lett.* **2010**, *10*, 3062−3067.
(80) Sewall, S. L.; Franceschetti, A.; Cooney, R. R.; Zunger, A.; Kambhampati, P. *Phys. Rev. B* **2009**, *80*, 081310(R).
(81) Sewall, S. L.; Cooney, R. R.; Kambhampati, P. *Appl. Phys. Lett.* **2009**, *94*, 243116−243113.
(82) Sagar, D. M.; Cooney, R. R.; Sewall, S. L.; Kambhampati, P. *J. Phys. Chem. C* **2008**, *112*, 9124−9127.
(83) Sagar, D. M.; Cooney, R. R.; Sewall, S. L.; Dias, E. A.; Barsan, M. M.; Butler, I. S.; Kambhampati, P. *Phys. Rev. B* **2008**, *77*, 235321−235314.
(84) Anderson, K. E. H.; Sewall, S. L.; Cooney, R. R.; Kambhampati, P. *Rev. Sci. Instrum.* **2007**, *78*, 073101−073106.
(85) Sewall, S. L.; Cooney, R. R.; Anderson, K. E. H.; Dias, E. A.; Kambhampati, P. *Phys. Rev. B* **2006**, *74*, 235328.
(86) Kippeny, T. C.; Bowers, M. J.; Dukes, A. D.; McBride, J. R.; Orndorff, R. L.; Garrett, M. D.; Rosenthal, S. J. *J. Chem. Phys.* **2008**, *128*, 084713.
(87) Garrett, M. D.; Dukes, A. D.; McBride, J. R.; Smith, N. J.; Pennycook, S. J.; Rosenthal, S. J. *J. Phys. Chem. C* **2008**, *112*, 12736−12746.
(88) Garrett, M. D.; Bowers, M. J.; McBride, J. R.; Orndorff, R. L.; Pennycook, S. J.; Rosenthal, S. J. *J. Phys. Chem. C* **2008**, *112*, 436−442.
(89) Underwood, D. F.; Kippeny, T.; Rosenthal, S. J. *J. Phys. Chem. B* **2001**, *105*, 436−443.
(90) Sykora, M.; Koposov, A. Y.; McGuire, J. A.; Schulze, R. K.; Tretiak, O.; Pietryga, J. M.; Klimov, V. I. *ACS Nano* **2010**, *4*, 2021−2034.
(91) McGuire, J. A.; Joo, J.; Pietryga, J. M.; Schaller, R. D.; Klimov, V. I. *Acc. Chem. Res.* **2008**, *41*, 1810−1819.
(92) McGuire, J. A.; Sykora, M.; Robel, I.; Padilha, L. A.; Joo, J.; Pietryga, J. M.; Klimov, V. I. *ACS Nano* **2010**, *4*, 6087−6097.
(93) Efros, A. L.; Rosen, M. *Phys. Rev. Lett.* **1997**, *78*, 1110−1113.
(94) Empedocles, S. A.; Neuhauser, R.; Shimizu, K.; Bawendi, M. G. *Adv. Mater.* **1999**, *11*, 1243−1256.
(95) Son, D. H.; Wittenberg, J. S.; Banin, U.; Alivisatos, A. P. *J. Phys. Chem. B* **2006**, *110*, 19884−19890.
(96) Son, D. H.; Wittenberg, J. S.; Alivisatos, A. P. *Phys. Rev. Lett.* **2004**, *92*, 127406/127401−127406/127404.
(97) Burda, C.; Link, S.; Green, T. C.; El-Sayed, M. A. *J. Phys. Chem. B* **1999**, *103*, 10775−10780.
(98) Norris, D. J.; Efros, A. L.; Rosen, M.; Bawendi, M. G. *Phys. Rev. B* **1996**, *53*, 16347−16354.
(99) Norris, D. J.; Bawendi, M. G. *Phys. Rev. B* **1996**, *53*, 16338−16346.
(100) Efros, A. L.; Rosen, M. *Phys. Rev. B* **1998**, *58*, 7120−7135.
(101) Zhong, H.; Nagy, M.; Jones, M.; Scholes, G. D. *J. Phys. Chem. C* **2009**, *113*, 10465−10470.
(102) McArthur, E. A.; Morris-Cohen, A. J.; Knowles, K. E.; Weiss, E. A. *J. Phys. Chem. B* **2010**, *114*, 14514−14520.

(103) An, J. M.; Franceschetti, A.; Dudiy, S. V.; Zunger, A. *Nano Lett.* **2006**, *6*, 2728−2735.
(104) Harbold, J. M.; Du, H.; Krauss, T. D.; Cho, K.-S.; Murray, C. B.; Wise, F. W. *Phys. Rev. B* **2005**, *72*, 195312/195311−195312/195316.
(105) Kang, I.; Wise, F. W. *J. Opt. Soc. Am. B* **1997**, *14*, 1632−1646.
(106) Schaller, R. D.; Pietryga, J. M.; Goupalov, S. V.; Petruska, M. A.; Ivanov, S. A.; Klimov, V. I. *Phys. Rev. Lett.* **2005**, *95*, 196401/196401−196401/196404.
(107) Hu, Y. Z.; Koch, S. W.; Lindberg, M.; Peyghambarian, N.; Pollock, E. L.; Abraham, F. F. *Phys. Rev. Lett.* **1990**, *64*, 1805−1807.
(108) Kelley, A. M. *J. Phys. Chem. Lett.* **2010**, *1*, 1296−1300.
(109) Barbara, P. F.; Meyer, T. J.; Ratner, M. A. *J. Phys. Chem.* **1996**, *100*, 13148−13168.
(110) Jones, M.; Lo, S. S.; Scholes, G. D. *J. Phys. Chem. C* **2009**, *113*, 18632−18642.
(111) Jones, M.; Lo, S. S.; Scholes, G. D. *Proc. Natl. Acad. Sci. U.S.A.* **2009**, *106*, 3011−3016.
(112) Jones, M.; Kumar, S.; Lo, S. S.; Scholes, G. D. *J. Phys. Chem. C* **2008**, *112*, 5423−5431.
(113) Mooney, J.; Krause, M. M.; Saari, J. I.; Kambhampati, P. 2012, submitted for publication.
(114) Babentsov, V.; Riegler, J.; Schneider, J.; Fiederle, M.; Nann, T. *J. Phys. Chem. B* **2005**, *109*, 15349−15354.
(115) de Mello Donegá, C.; Bode, M.; Meijerink, A. *Phys. Rev. B* **2006**, *74*, 085320.